Journal of Biomolecular NMR (2006) 36: 27–36
DOI 10.1007/s10858-006-9063-4

Article

Measurement of ^{15}N relaxation in deuterated amide groups in proteins using direct nitrogen detection

Paul R. Vasos[a], Jennifer B. Hall[a], Rainer Kümmerle[b] & David Fushman[a,*]
[a]*Department of Chemistry and Biochemistry, Center for Biomolecular Structure and Organization, University of Maryland, 1115 Biomolecular Sciences Building (#296), College Park, MD 20742-3360 USA;* [b]*Bruker Biospin AG, NMR Division, Industriestrasse 26, CH-8117 Fällanden, Switzerland*

Received 18 April 2006; Accepted 30 June 2006

Key words: chemical shielding anisotropy, CSA, direct nitrogen detection, heteronuclear NMR, protein G, spin relaxation

Abstract

^{15}N chemical shielding tensors contain useful structural information, and their knowledge is essential for accurate analysis of protein backbone dynamics. The anisotropic component (CSA) of ^{15}N chemical shielding can be obtained from ^{15}N relaxation measurements in solution. However, the predominant contribution to nitrogen relaxation from ^{15}N–^{1}H dipolar coupling in amide groups limits the sensitivity of these measurements to the actual CSA values. Here we present nitrogen-detected NMR experiments for measuring ^{15}N relaxation in deuterated amide groups in proteins, where the dipolar contribution to ^{15}N relaxation is significantly reduced by the deuteration. Under these conditions nitrogen spin relaxation becomes a sensitive probe for variations in ^{15}N chemical shielding tensors. Using the nitrogen direct-detection experiments we measured the rates of longitudinal and transverse ^{15}N relaxation for backbone amides in protein G in D_2O at 11.7 T. The measured relaxation rates are validated by comparing the overall rotational diffusion tensor obtained from these data with that from the conventional ^{15}N relaxation measurements in H_2O. This analysis revealed a 17–24° angle between the NH-bond and the unique axis of the ^{15}N chemical shielding tensor.

Abbreviations: CSA – chemical shielding anisotropy; NMR – nuclear magnetic resonance.

Introduction

NMR measurements can provide a wealth of information about structure and dynamics in biomolecules. Current challenges in the use of NMR to study dynamics include (1) extending the time window accessible by the available methods and (2) finding accurate and robust solutions to an underdetermined problem: a multitude of interaction and motional parameters (dipolar coupling constants, chemical shielding tensors, characteristics of the overall and local motions) have to be obtained from the few existing experiments. In particular, the widely performed analysis of local motions in the protein backbone from ^{15}N relaxation data requires knowledge of structure-related parameters, the N–H bond length and the anisotropy (CSA) of the ^{15}N chemical shielding tensor. Recent studies have shown that the ^{15}N CSA could vary from site to site in proteins (Fushman et al., 1998, 1999; Kroenke et al., 1999; Kover and Batta, 2001; Damberg et al., 2005; Hall and Fushman, 2006), therefore its knowledge is essential for an

*To whom correspondence should be addressed. E-mail: fushman@umd.edu

accurate picture of protein dynamics (Fushman and Cowburn, 2001). While ^{15}N CSA values can be obtained by combining relaxation measurements at several fields (Fushman and Cowburn, 2001; Hall and Fushman, 2006), the accuracy and precision of such analysis could be limited by the fact that the CSA contribution to ^{15}N relaxation is markedly lower than the dipolar contribution, at magnetic fields currently available. For example, the CSA mechanism contributes only 12% of the ^{15}N transverse relaxation rate at 9.4 T, and even at 21.1 T its contribution is about 41% (for a protein with a rotational correlation time of 5 ns and assuming CSA = -160 ppm).

Here we introduce the use of heteronuclear-detected experiments to measure the ^{15}N relaxation rates in proteins in D_2O, where the dipolar contribution is lessened by replacing the dipolar-coupled partner (^1H) with a deuteron. In the case of ^{15}N-only labeled proteins in D_2O, the nitrogen nucleus remains an isolated and convenient probe for motion, provided the dynamic characteristics of the ^{15}N–^1H and ^{15}N–^2H vectors (referred to here as NH and ND, respectively) are similar. Although the fast NH bond librations might be affected by the $^1H \rightarrow {}^2H$ replacement, the motions of the peptide planes and larger-scale segmental motions – the major contributors to NMR-detected local dynamics in the backbone (Fushman et al., 1994; Pfeiffer et al., 2001) – are expected to be much less sensitive to the deuteration. Because ^{15}N CSA is the major mechanism of ^{15}N relaxation in the ND spin pair, the proposed measurements could provide a more sensitive probe for determining ^{15}N CSA tensors (see below). In addition, this method has the potential of extending the current repertoire of spectral densities sampled by ^{15}N relaxation measurements, as the relaxation rates in the ND spin system are sensitive to motional averaging at different frequencies than in the NH pair (Xu et al., 2005).

The lower sensitivity of nitrogen detection compared to proton detection can be compensated, at least in part, by the use of specially designed probes (Bertini et al., 2004a). In addition, the ^{15}N signals are significantly sharper than ^1H signals, which would partially recover the loss in sensitivity. When fast-relaxing systems are studied, it becomes increasingly common to make use of the early techniques employing heteronuclei for the starting magnetization and the signal detection (Oh et al., 1988). Recently, it has been shown that pulse sequences using ^{13}C detection are more sensitive than the classical ^1H-detected ones in the presence of fast relaxation induced by a paramagnetic center (Bermel et al., 2003). This has triggered the development of ^{13}C detection methods for applications to large proteins (Eletsky et al., 2003; Bertini et al., 2004b; Vogeli et al., 2004).

Results and discussion

The measurements were performed on a 5.8 mM sample of protein G (GB3) (Hall and Fushman, 2003) in D_2O at 11.7 T and 24 °C, on a 5 mm Z-Gradient P/C/N–H/D QNP CryoProbe. This is a double resonance observe-type probehead. The inner coil can be switched between ^{31}P, ^{13}C and ^{15}N, the decoupling coil is tuned to ^1H. The ^2H channel can be used for lock, decoupling (as in our measurements) and for direct observation. The probehead is fitted with cryogenically cooled preamplifiers for all nuclei. The cooled ^{15}N RF coil and preamplifier in the QNP probe offer a 4-fold gain in sensitivity compared to conventional broadband and QNP probeheads and an approximately similar sensitivity increase with respect to the TXI or TCI cryoprobes using room-temperature ^{15}N preamplifiers. Our data indicate that the proposed measurements are feasible using conventional broadband and cryo-TXI probes, on fairly concentrated protein samples. The replacement of the amide proton with a deuteron is expected to result in considerably sharper ^{15}N lines, thereby enhancing both the signal-to-noise and the resolution in the observed spectra. For small-size proteins, the 1D spectra provide reasonable resolution for individually fitting the signals from the majority of residues. In the case of GB3, 51 out of the 55 assigned signals from the backbone amides, as well as the signal of the indole group of Trp43, could be resolved (Figure 1). Deuterium and proton decoupling was applied during the acquisition, resulting in linewidths of ≤ 1 Hz (and down to 0.7 Hz in some signals). For comparison, ^{15}N linewidths of ≥ 3 Hz were observed in a ^{15}N-detected spectrum of protonated ubiquitin in H_2O.

The ^{15}N relaxation rates R_2 and R_1 were measured using the pulse sequences in Figure 2, the representative fitting curves are shown in Figure 3. The ^{15}N relaxation data are depicted in Figure 4 as

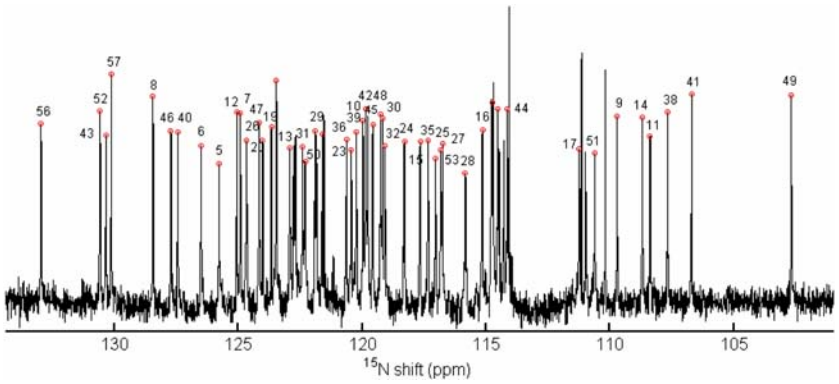

Figure 1. ^{15}N-detected spectrum of GB3 (pH 5.5, 24 °C), recorded at 11.7 T with 5k scans and a recycle delay of 3.5 s (total time 5 h). The acquisition time was 0.92 s, no apodization was applied during processing. The residue numbers are indicated at the frequency position of the corresponding ^{15}N resonance. All the assigned signals originating from backbone amides that could be resolved are labeled with the residue number, the indole signal of Trp43 is labeled 57. Circles without labels correspond to signals in overlap.

a function of residue number. The profile is similar to that of the relaxation data in H_2O (Hall and Fushman, 2003), i.e. relaxation rates in the α-helix are higher than those measured in the rest of the protein (see also Figure 5), although the difference is not as striking as for the H_2O data (see below). The analysis of ^{15}N relaxation data in H_2O led to the conclusion (Hall and Fushman, 2003) that the elevated ^{15}N R_2 values in the helix reflect anisotropy of the overall tumbling of GB3. In support of that conclusion, the current data indicate that elevated relaxation rates of amide nitrogens in the helix are not due to higher CSA values, otherwise the difference would have become more pronounced in the data recorded in D_2O. The low values of both relaxation rates in the β1/β2 and α/β3 loops are due to increased mobility in these regions.

Overall rotational diffusion tensor

In order to validate the relaxation data obtained by ^{15}N direct detection, we used them to determine the overall rotational diffusion tensor of GB3. This was done using the computer program ROTDIF (Walker et al., 2004) that fits the ratio of experimentally measured ^{15}N relaxation rates:

$$\rho = \left(\frac{2R_2'}{R_1'} - 1\right)^{-1}, \tag{1}$$

to the value predicted from theory. The primes in Equation 1 indicate "reduced" relaxation rates, usually obtained by subtracting the components of the spectral density involving proton frequency (in the NH pair). The advantage of this method is that the ratio ρ is independent, to a first approximation, of the ^{15}N CSA values and of the order parameters describing local backbone motion (Fushman and Cowburn, 2002). To adapt this method to ND systems, the spectral densities $J(\omega)$ at frequencies involving deuterium frequency (ω_D, $\omega_D \pm \omega_N$) were subtracted from the measured R_1 and R_2 values as follows:

$$R_1' = R_1 - \frac{8}{3}d^2[6J(\omega_D + \omega_N) + J(\omega_D - \omega_N)], \tag{2a}$$

$$R_2' = R_2 - \frac{4}{3}d^2[6J(\omega_D) + 6J(\omega_D + \omega_N) + J(\omega_D - \omega_N)], \tag{2b}$$

where $d = -\frac{1}{2}\frac{\mu_0}{4\pi}\frac{\hbar\gamma_N\gamma_D}{r^3_{ND}}$ is the dipolar coupling constant in the ND pair. The spectral densities were calculated using the model-free assumption (Lipari and Szabo, 1982), as detailed in Supporting Material. As shown in (Xu et al., 2005), the model-free form of the spectral density is applicable to ND bond dynamics in deuterated amides. Axial symmetry was assumed for the overall rotational diffusion tensor of GB3. As shown elsewhere (Hall and Fushman, 2003), a more complex, fully anisotropic diffusion model is not warranted for GB3. The orientations of the NH vectors were taken from the crystal structure (PDB entry 1IGD

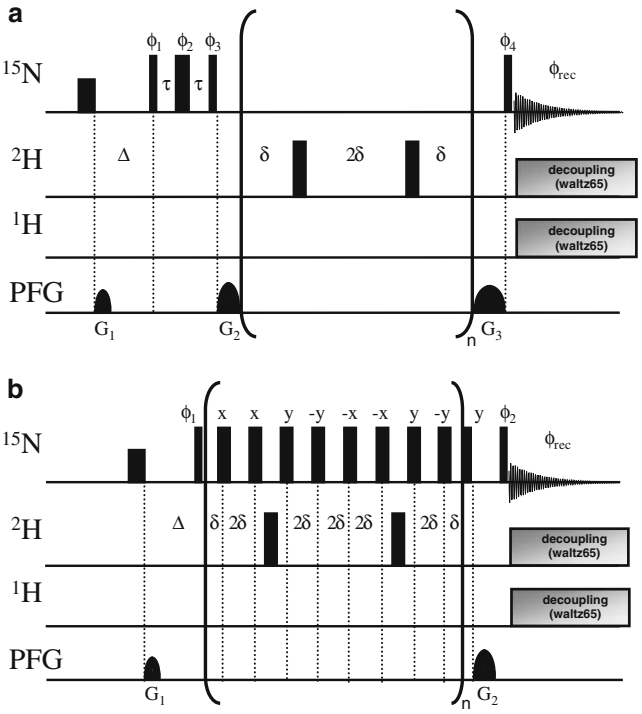

Figure 2. Pulse sequences for 1D ^{15}N-detected (a) R_1 and (b) R_2 measurements. Narrow and wide bars indicate 90° and 180° pulses, respectively, applied along the *x*-axis unless specified otherwise. The relaxation delays for the R_1 experiments were 11.15, 105.84, 209.13, 295.21, 398.51 (*x*2), 605.1, 794.48 and 1001.07 ms and for the R_2 experiments 3.74, 103.10, 198.78 (*x*2), 265.02, 323.90, 397.50 and 449.02 ms. The pulse repetition delays δ were of 2 ms and 200 μs in the R_1 and R_2 experiments, respectively. The delay τ was 10 μs. The phases were: $\phi_1 = (y,-y)$, $\phi_2 = (8x,8(-x))$, $\phi_3 = (2(-y),2y)$, $\phi_4 = (4x,4(-x))$ and $\phi_{rec} = (x,2(-x),x,-x,2x,-x)$ in the R_1 experiment and $\phi_1 = (y,-y)$, $\phi_2 = (2x,2(-x))$ and $\phi_{rec} = (x,2(-x),x)$ in the R_2 experiment (the latter phase cycle is based on a recently published modification of the CPMG experiment (Yip and Zuiderweg, 2004)). Sine-bell shaped gradients with a duration of 1 ms and ratios of intensities of $G_1{:}G_2{:}G_3 = -5{:}2{:}1.4$ and $G_1{:}G_2 = -5{:}2$ were used in the R_1 and R_2 experiments, respectively. The number of scans was from 4k to 8k, depending on the total relaxation period. The acquisition time was 300 ms. Waltz65 decoupling was applied during the acquisition on the ^{1}H and ^{2}H channels; this consists of an MLEV4 supercycle of the basic waltz16 element (waltz64) with an additional 90° pulse at the end of the supercycle for increased performance with respect to decoupling sidebands. ^{15}N pulses were applied at 16.6 kHz, while the ^{2}H decoupling was at a power level of 880 Hz. A low-power 90° pulse followed by a gradient was applied at the beginning of the sequences in order to defocus the ^{15}N magnetization prior to the relaxation period. The ^{2}H spectrometer lock was kept on during the relaxation period Δ (2.9 s) and switched off just prior to the first rf pulse. The scalar relaxation of the second kind was suppressed using deuterium decoupling (Xu et al., 2005). Note that, strictly speaking, these pulse sequences are designed for fully deuterated proteins. Applications to protonated proteins in D_2O could require proton decoupling during the relaxation period, to suppress possible contributions from cross-correlation between ^{15}N CSA and dipolar coupling to ''other'' protons, e.g. H_α. Our data (not shown) indicate that in GB3 the T_1 values measured with and without such a decoupling are similar within the experimental errors.

(Derrick and Wigley, 1994)), and the backbone model-free parameters were obtained from a multiple-field analysis of relaxation data (Hall and Fushman, 2006). The ND bond length was set to 1.02 Å. Note that the subtracted $J(\omega)$ components (Equations 2) and the R_2'/R_1' ratio both are, to a first approximation, independent of the magnitude of ^{15}N CSA, therefore the diffusion tensor can be derived without making any assumption regarding the CSA values (Fushman and Cowburn, 2002; Walker et al., 2004). The calculation of the $J(\omega)$ components to be subtracted in Equations 2 was performed using the diffusion tensor determined from ^{15}N relaxation data for GB3 in H_2O (Hall and Fushman, 2003) at 14.1 T (Table 1, first row). The principal values of the diffusion tensor were scaled by 0.81 to account for higher shear viscosity of D_2O compared to H_2O (Cho et al., 1999). In

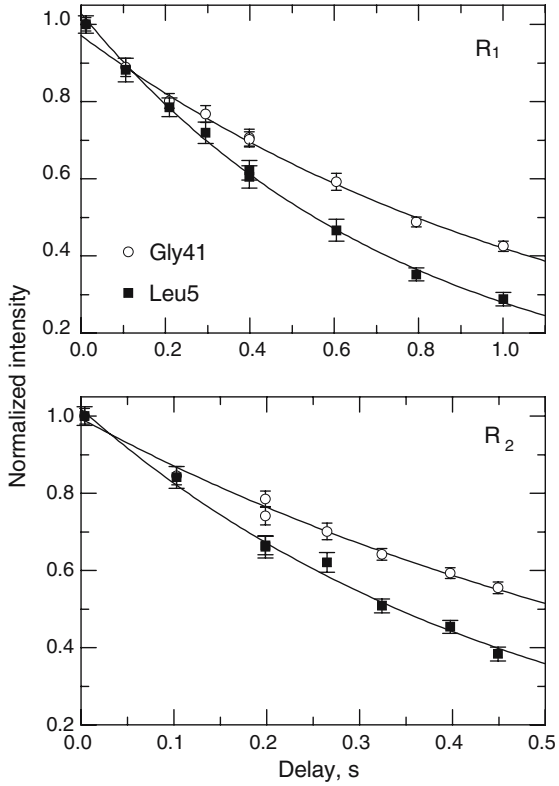

Figure 3. Representative fitting curves for R_1 and R_2 measurements are shown for Leu5 and Gly41, as indicated. Peak intensities in a series of 1D spectra recorded with different relaxation delays were fit to a mono-exponential decay. The error bars represent experimental errors in peak intensities estimated from noise integration.

addition to this partial subtraction of the spectral densities associated with N–D dipolar interaction, a second calculation was performed in which the entire dipolar contribution to the relaxation rates was subtracted, as follows:

$$R_1' = R_1 - 8d^2 J(\omega_N) - \frac{8}{3}d^2[6J(\omega_D + \omega_N) + J(\omega_D - \omega_N)], \quad (3a)$$

$$R_2' = R_2 - \frac{4}{3}d^2[4J(0) + 3J(\omega_N)] - \frac{4}{3}d^2[6J(\omega_D) + 6J(\omega_D + \omega_N) + J(\omega_D - \omega_N)], \quad (3b)$$

The calculations using Equations 2 and 3 both yielded similar anisotropies and orientations for the diffusion tensor (Table 1). Moreover, these results are in good agreement with those determined from ^{15}N relaxation rates measured in H_2O using conventional methods (Table 1, also (Hall and Fushman, 2003)). The observed slower tumbling of GB3 in D_2O (τ_c = 4.2 – 4.3 ns versus 3.3 ns in H_2O) is consistent with a 1.25-fold higher viscosity of this solvent. This tumbling time also agrees with the value of 4.55 ± 0.24 ns obtained from ^{15}N relaxation data (not shown) measured for the residual NH groups (approximately 2–3%) in this GB3 sample in D_2O using conventional INEPT-based 2D methods. Note also the self-consistency of the diffusion tensor determination procedure used here: the output τ_c value from the ROTDIF calculation agrees well with the input value used for the subtraction of dipolar contributions in Equations 2 and 3.

Note that the choice between Equations 2 and 3 for practical use depends on the purpose of analysis. Equations 2 involve less assumptions and, therefore, are preferred, particularly when the goal is to subtract the $J(\omega)$ components involving deuterium frequency, in order to obtain "reduced" relaxation rates, as is done in the case of NH-pairs by subtraction of the high-frequency components (e.g., (Fushman and Cowburn, 1998)). However, if the goal is to remove the dipolar contribution entirely, hence to have the CSA-only terms, then Equations 3 should be used.

Orientation of the CSA tensor

We have used the ^{15}N relaxation data in ND systems to explore the orientation of the CSA tensor. The determination of the diffusion tensor of a protein from ^{15}N relaxation data rests on the dependence of the relaxation rates on the angles between the principal axes of this tensor and the symmetry axis of the relaxation-active terms in the spin Hamiltonian. The latter axis is usually assumed to be the same for all terms and pointing in the direction (averaged by fast local motion) of the NH bond, because the ^{15}N–^{1}H dipolar coupling is the primary interaction governing ^{15}N relaxation. In the case of the ND spin system, the CSA contribution is dominant (see below) and therefore the orientation of the ^{15}N CSA tensor becomes the determining factor for the ^{15}N relaxation rates. Because the chemical shift is sensitive to the local distribution of electron density, the ^{15}N CSA tensor's orientation is in general different from that of the NH-bond vector (corrections for

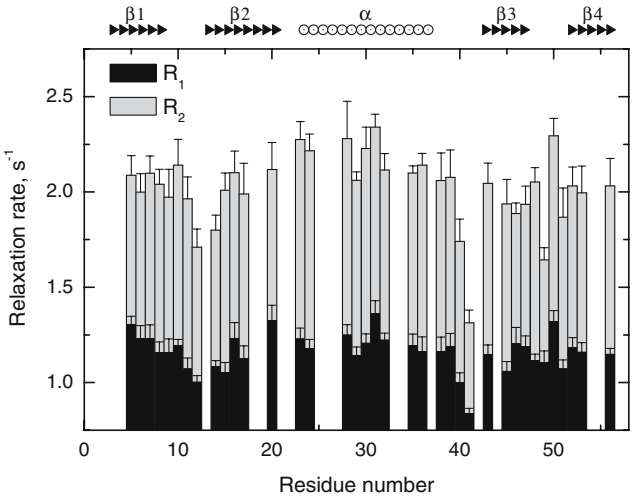

Figure 4. Longitudinal (R_1, black bars) and transverse (R_2, grey bars) ^{15}N relaxation rates in GB3 in D_2O, determined using ^{15}N direct detection at 11.7 T (500 MHz ^{1}H frequency). The diagram on the top indicates the location of the secondary structure elements.

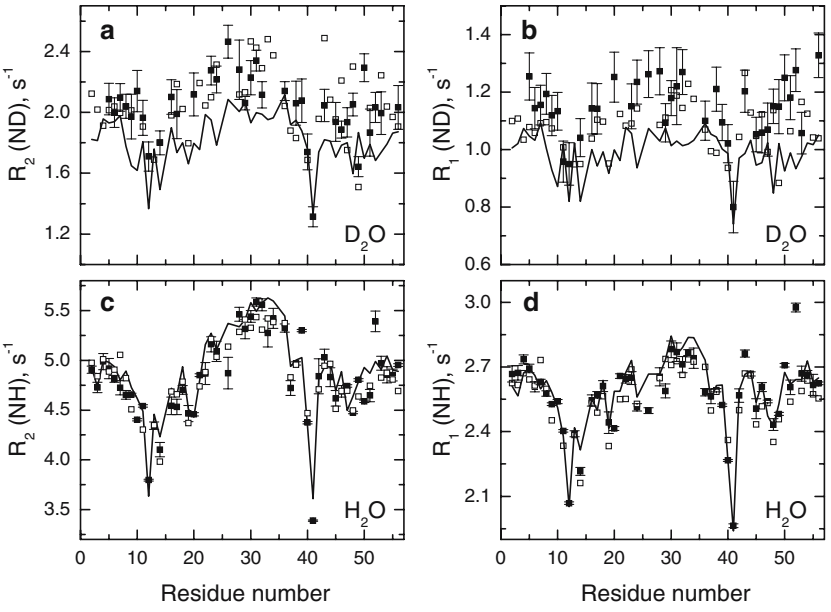

Figure 5. The agreement between experimental (solid squares) and calculated ^{15}N R_2 and R_1 values for (a,b) ND groups (in D_2O) and (c,d) NH groups (in H_2O) in GB3 at 11.7 T. The calculated data were obtained using model-free spectral densities and assuming uniform ^{15}N CSA of -160 ppm (solid line) or using site-specific ^{15}N CSA values (open squares) obtained from five-field analysis and ranging from -131 (Thr49) to -216 ppm (Ala48) (Hall and Fushman, 2006). The site-specific CSA data are not included for Leu12, Ala20, Ala26, and Phe52, which were outliers in that study. The overall rotational diffusion tensors of GB3 in H_2O and D_2O were as in Table 1, the model-free parameters were from multiple-field data analysis (Hall and Fushman, 2006). The contributions from remote protons are included in (a,b); but not included in (c,d) (in keeping with standard practice) since this effect is negligible compared to the dipolar coupling between the ^{15}N nucleus and the bound ^{1}H.

the noncollinearity between the two interactions are discussed in (Fushman and Cowburn, 1999)). The anisotropy of local backbone motions could also contribute to the difference between average orientations of the CSA and dipolar tensors. To account for the possible difference in the

Table 1. Characteristics of the overall rotational diffusion tensor of GB3 determined from ^{15}N relaxation data measured by the direct method proposed here and by conventional relaxation approaches

Spin pair	$J(\omega)$ components subtracted	β^a	ξ^a	τ_c^b	$D_\parallel/D_\perp^b$	Φ^c	Θ^c
^{15}N–^{1}H (sample in H_2O)	$J(\omega_H)$, $J(\omega_H \pm \omega_N)$	0^d	0^d	3.3 (0.1)	1.4 (0.1)	92 (6)	72 (7)
		-3^e	0^e	3.3 (0.1)	1.4 (0.1)	95 (6)	68 (7)
^{15}N–^{2}H (sample in D_2O)	$J(\omega_D)$, $J(\omega_D \pm \omega_N)$	0^d	0^d	4.2 (0.4)	1.3 (0.2)	103 (28)	68 (23)
		17^e	2^e	4.2 (0.4)	1.3 (0.2)	96 (26)	75 (21)
	$J(0)$, $J(\omega_N)$, $J(\omega_D)$, $J(\omega_D \pm \omega_N)$	0^d	0^d	4.3 (0.5)	1.3 (0.3)	105 (34)	66 (29)
		24^e	3^e	4.3 (0.4)	1.3 (0.3)	98 (26)	77 (23)

Numbers in the parentheses represent standard deviations. [a]The angles β and ξ (in degrees) correspond to a tilt of the interaction axis away from the NH bond (see text). [b]The overall correlation time $\tau_c = 1/[2(D_\parallel + 2D_\perp)]$ (in nanoseconds) and the anisotropy, $D_\parallel/D_\perp$, of the diffusion tensor. [c]The angles Φ and Θ (in degrees) determine the orientation of unique axis of the rotational diffusion tensor with respect to the protein coordinate frame. [d]The angles β and ξ were fixed at 0, i.e. the interaction axis was assumed to be in the direction of the N–H bond. [e]The angles β and ξ were adjusted as a result of a grid search minimizing the residuals of fit.

orientations of the relaxation-active interaction and the NH vector, we allowed the former to deviate from the NH bond in both in-plane and out-of-plane directions using two degrees of freedom described by the angles β and ξ. The angle β measured the deviation of the interaction frame from the NH orientation in the peptide plane, with the positive direction towards the carbonyl nucleus of the previous residue. The angle ξ measured the deviation away from the peptide plane, with the positive sign corresponding to a clockwise rotation about the N–H bond (when looking from H to N). The tilt of the interaction axis was assumed to be the same for all residues in the protein. The ROTDIF analysis (see above) was performed on a $\{\beta, \xi\}$ grid, and the resulting values of the target function obtained from all grid points were compared, in order to find the orientation of the axis that minimizes the difference between the experimental and back-calculated values of ρ. Note that in this analysis we assume that the relaxation–relevant interaction is axially symmetric, i.e. can be characterized by a unique axis. While clearly an approximation, this assumption is accurate when the dipolar coupling is the dominant interaction and also seems a reasonable first approximation in the case of relaxation dominated by the CSA mechanism, due to relatively small deviations of ^{15}N chemical shielding tensors in proteins from axial symmetry (Cornilescu and Bax, 2000; Loth et al., 2005; Wylie et al., 2006).

Using reduced relaxation rates (Equations 2), the optimal orientation of the axis of interaction was found to be approximately in the peptide plane and titled by 17° from the NH-vector towards the carbonyl atom (Table 1, Figure 6). This result prompted us to further investigate the hypothesis that the orientation of the principal frame of the relaxation–active interaction in the N–D pair reflects the dominant (in this case) contribution from the ^{15}N CSA interaction (assumed axially symmetric). In order to explore this, the dipolar contribution was entirely subtracted from the relaxation rates (see above). This resulted in a further increase, to 24°, in the tilt angle β in the same direction of rotation. Given the relatively broad minimum of the target function versus angle β, these numbers are in good agreement with one another. Note also that the characteristics of the rotational diffusion tensor obtained at these optimal values of the tilt angles agree for the two subtraction methods and with those measured in NH groups in GB3 using conventional methods (Table 1). Although the reduction in χ^2 compared to the zero-tilt model is not dramatic, likely reflecting the limited precision of the data, the statistical *F*-test gave confidence levels of 83 and 85%, respectively, for the two cases. The out-of-plane tilt angle ξ was small (2°–3°) and statistically not significant. The slight increase in the tilt angle when the dipolar contribution to relaxation was completely subtracted agrees with the idea that the observed behavior is the result of an interplay between the orientations of the dipolar and CSA interactions. In a control analysis of ^{15}N relaxation data for GB3 in H_2O (at 14.1 T), the minimum was found within 3° of the NH vector orientation (Figure 6), as expected because of the predominant contribution to ^{15}N relaxation from dipolar coupling in the NH pair.

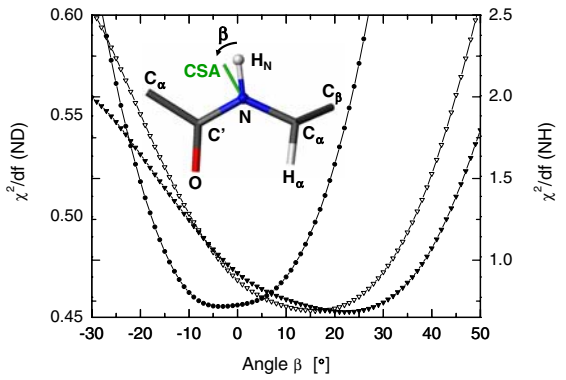

Figure 6. Variation in the residuals of the fit (from ROTDIF analysis), as the main interaction frame is tilted away from the direction of the NH vector, while remaining in the peptide plane (angle $\xi = 0$). Shown is the value of the target function per degree of freedom (χ^2/df) from a least-square fit of experimental data (Equation 1) assuming axially symmetric overall rotational diffusion tensor. The curves correspond to subtraction of the dipolar contributions at frequencies containing combinations of the deuterium Larmor frequency (Equations 2, open triangles) and at all frequencies (Equations 3, solid triangles). Shown for comparison (solid circles) are the results of a similar analysis of ^{15}N relaxation data in NH-pairs (in H_2O). The left-hand y-axis scale corresponds to χ^2/df for both sets of D_2O data while the right-hand y-axis scale is for the ^{1}H-detected ^{15}N relaxation data collected for the GB3 sample in H_2O. A schematic representation of the orientation of the CSA tensor axis at the position of minimum χ^2 is shown in the insert.

Because ^{15}N CSA is the dominant mechanism of ^{15}N relaxation in ND pairs under these conditions, this analysis provides the average orientation of the ^{15}N CSA tensor. Indeed, the derived values of the in-plane tilt angle β are in good agreement with both solid-state NMR data on short peptides (summarized in (Korzhnev et al., 2001)) and solution NMR measurements in ubiquitin (Fushman et al., 1998; Cornilescu and Bax, 2000; Kurita et al., 2003; Damberg et al., 2005; Loth et al., 2005) which give a range from 13° to 26° (and the mean values from 16° to 21°) for the angle between the NH-bond and the least-shielded component of the CSA tensor, in the peptide plane.

The deviation of the average orientation of the CSA tensor from that of the NH bond explains the fact that the R_2 values in the α-helix (residues 23–36, Figures 4, 5b) are less elevated relative to the rest of the protein than in H_2O (Figure 5b) (Hall and Fushman, 2003). As shown in (Hall and Fushman, 2003), the elevated R_2s in the α-helix are the result of the unique principal axis of the diffusion tensor of GB3 being approximately parallel to the helix axis (hence to NH vectors in the helix) and approximately perpendicular to NH vectors in the β-sheet. The effect is less pronounced in D_2O, because the CSA tensors – the main contributors to ^{15}N relaxation – in the β-sheet are tilted from the NH vectors and therefore are better aligned with the diffusion tensor axis (a 17° tilt of the CSA in the peptide plane corresponds to an average 10° tilt *towards* the diffusion tensor for β-sheet residues). The CSA tensors in the α-helix, on the other hand, are correspondingly less well aligned with the helix axis (and therefore with the diffusion tensor axis) than their NH vectors due to this same tilt, the combined effect being that there is less of an elevation of transverse relaxation rates in the helix with respect to those in the β-sheet (cf. Figure 5a and b).

Sensitivity to site-specific CSA variations

The advantage of ^{15}N relaxation measurements in ND systems is in their higher relative sensitivity to ^{15}N CSA compared to the conventional measurements in H_2O. Consider for example CSA determination from the field dependence (Fushman et al., 1999; Fushman and Cowburn, 2001) of

$$2R_2 - R_1 = \frac{8}{3}d^2[4J(0) + 6J(\omega_D)] + 4(\omega_N \cdot \Delta\sigma/3)^2 J(0), \quad (4)$$

where $|\Delta\sigma| = \left[\sigma_{xx}^2 + \sigma_{yy}^2 + \sigma_{zz}^2 - (\sigma_{xx}\sigma_{yy} + \sigma_{xx}\sigma_{zz} + \sigma_{yy}\sigma_{zz})\right]^{1/2}$ is a general expression (Canet, 1998) for the effective anisotropy of the chemical shielding tensor $\underline{\underline{\sigma}}$; which reduces to the more conventional one, $\Delta\sigma = \sigma_\parallel - \sigma_\perp$, in the case of axially symmetric tensor ($\sigma_{xx} = \sigma_{yy} = \sigma_\perp, \sigma_{zz} = \sigma_\parallel$). At 11.7 T, the ratio of relative contributions from the dipolar interaction and ^{15}N CSA is greater than 4:1 in NH systems but changes drastically to approximately 1:3 in ND pairs, i.e. the overall gain is ~12 fold. These numbers vary only slightly as a function of the protein size. Overall, a 10% variation in the CSA will result in a ~7.5% variation in $2R_2 - R_1$ (ND-pair) compared to only a ~2% effect for the NH pair. Naturally, the CSA contribution to ^{15}N relaxation increases with the field and in ND systems exceeds 90% at 21.1 T. This suggests a higher accuracy of CSA determination from ^{15}N relaxation measurements in ND systems.

Indeed, as illustrated in Figure 5, the experimental R_2 values in ND systems are in a markedly better agreement with the predictions based on site-specific ^{15}N CSAs than with those for a constant CSA of -160 ppm, whereas the R_2 values measured in H_2O are not sensitive enough to discriminate between uniform and site-specific ^{15}N CSA values. The sensitivity of the presented method to variations in the ^{15}N CSA values and to the orientation of the CSA tensor is an unprecedented feature, permitting the determination of the orientation of the CSA tensor along with the rotational diffusion tensor. The availability of ^{15}N-detected relaxation data at several fields would allow us to quantify the ^{15}N CSA values using the field-dependence of the combinations of relaxation rates (work in progress) – similar approaches were developed for ^{15}N relaxation data measured in H_2O (Fushman and Cowburn, 2001).

In addition to their sensitivity to the ^{15}N CSA, relaxation measurements in ND systems offer certain advantages for detecting nanosecond and slower motions in proteins. First, these measurements extend the current repertoire of spectral densities sampled by ^{15}N relaxation measurements, as the relaxation rates in the ND spin system are sensitive to motional averaging at different frequencies than in the NH pair. Specifically, ^{15}N relaxation rates in ND systems sample the spectral density $J(\omega)$ at $\omega = 0$, ω_N, ω_D, and $\omega_N \pm \omega_D$, and it has been shown that at these frequencies the spectral density function describing motion of the ND bond is in agreement with that of the NH bond at higher frequencies (Xu et al., 2005). Due to the opposite signs and close absolute values of the gyromagnetic ratios of ^{15}N and ^{2}H $\omega_N + \omega_D$ is a relatively low frequency (21 MHz at 9.4 T and 42 MHz at 18.8 T), therefore knowledge of $J(\omega_N + \omega_D)$ has the potential to improve characterization of protein dynamics in the nanosecond timescale: $(\omega_N + \omega_D)^{-1} \approx 7.6$ ns at 9.4 T and 3.8 ns at 18.8 T. Combined with the other spectral density components, $J(\omega_N)$, $J(\omega_D)$, and $J(\omega_D - \omega_N)$, this will allow a detailed sampling/characterization of backbone motions in the range from 8 ns to 0.8 ns, which is important for understanding of motions in loops and other segments in a protein. It is worth mentioning in this regard that a proper combined analysis of backbone dynamics in NH and ND pairs requires that ^{15}N relaxation measurements for both groups be performed under the same sample viscosity conditions. This can be achieved by introducing a controlled amount of H_2O in the sample, as e.g. in (Xu et al., 2005), such that the NH measurements could be performed using the conventional inverse-detection methods. The pulse sequences in Figure 2 can be modified for these purposes by including prior to the acquisition a filter that suppresses signals originating from the (residual) protonated amides. Second, the total rate of ^{15}N transverse relaxation in ND pairs is substantially less than in NH pairs (due to the decrease in the dipolar contribution). This could improve NMR characterization of chemical exchange phenomena, as the quantification of these processes depends critically on the relative contribution of chemical exchange to the total transverse relaxation rate (Palmer et al., 2005).

A promising approach for exploiting the potential of the ^{15}N nucleus in the ^{15}N–^{2}H pair as a probe for motion has been proposed recently (Xu et al., 2005), based on indirect measurement of ^{15}N relaxation through magnetization transfer using HA(CACO)N-type experiment. Because of the ^{13}C enrichment required for that method, the ^{15}N–^{2}H system is not isolated, and corrections for contributions to ^{15}N relaxation caused by couplings with $^{13}C'$ and $^{13}C_\alpha$ are required for accurate analysis of the data. These contributions could be important, particularly at lower fields. With the protocol presented therein, the relaxation rates of the C_zN_+ antiphase coherence in ND systems are subtracted from those of NH systems. This subtraction, however, results in the loss of the information about the ^{15}N CSA contribution to relaxation. The direct way of measuring ^{15}N relaxation in the ^{15}N–^{2}H pair presented here is so far the only technique that analyzes the isolated ND pair, thus avoiding contributions from neighboring carbons. The relaxation rates observed are those of pure nitrogen coherences. As nitrogen magnetization is directly excited and detected, signals for all the residues can be acquired with this approach, including Pro and Gly. It is worth mentioning that the use of ^{15}N frequency for detection also circumvents the problems of suppressing the solvent signal.

Conclusions

In summary, we presented measurements of ^{15}N relaxation rates in a protein in D_2O using direct ^{15}N detection. These measurements became feasible due to hardware development. By sampling the spectral density function at the frequencies ω_D and $\omega_D \pm \omega_N$ these measurements provide potentially useful information about protein motions in the nanosecond time range not available from the conventional measurements in NH systems. In addition, the proposed direct ^{15}N-detection experiments offer increased sensitivity to ^{15}N CSA values and could provide a useful tool for accurate measurements of these parameters in proteins.

For small-size proteins, the 1D approach presented here offers good resolution because of the narrow lines. For larger-size proteins, where both spectral crowding and line broadening become critical, the ^{15}N detection approach could still be useful for quick determination of the overall tumbling time – using the average R_2 and R_1 values determined from the envelope of the spectrum (or its part). Heteronuclear direct-detection methods, avoiding magnetization transfer via fast-relaxing nuclei, have the potential of becoming useful when applied to large proteins or protein complexes.

Supplementary material

A figure showing a comparison of the 1D ^{15}N spectra obtained from ND and residual NH groups in the GB3 sample; a description of the procedure for calculating the spectral densities. This supplementary material is available at http://dx.doi.org/10.1007/s10858-006-9063-4.

Acknowledgements

Supported by NIH grant GM65334 to D.F.

References

Bermel, W., Bertini, I., Felli, I.C., Kummerle, R. and Pierattelli, R. (2003) *J. Am. Chem. Soc.*, **125**, 16423–16429.

Bertini, I., Felli, I.C., Kummerle, R., Moskau, D. and Pieratelli, R. (2004a) *J. Am. Chem. Soc.*, **126**, 464–465.

Bertini, I., Duma, L., Felli, I.C., Fey, M., Luchinat, C., Pierattelli, R. and Vasos, P.R. (2004b) *Angew. Chem. Int. Ed. Engl.*, **43**, 2257–2259.

Canet, D. (1998) *Concepts Magn. Reson.*, **10**, 291–297.

Cho, C.H., Urquidi, J., Singh, S. and Robinson, G.W. (1999) *J. Phys. Chem. B*, **103**, 1991–1994.

Cornilescu, G. and Bax, A. (2000) *J. Am. Chem. Soc.*, **122**, 10143–10154.

Damberg, P., Jarvet, J. and Graslund, A. (2005) *J. Am. Chem. Soc.*, **127**, 1995–2005.

Derrick, J.P. and Wigley, D.B. (1994) *J. Mol. Biol.*, **243**, 906–918.

Eletsky, A., Moreira, O., Kovacs, H. and Pervushin, K. (2003) *J. Biomol. NMR*, **26**, 167–179.

Fushman, D. and Cowburn, D. (1998) *J. Am. Chem. Soc.*, **120**, 7109–7110.

Fushman, D. and Cowburn, D. (1999) *J. Biomol. NMR*, **13**, 139–147.

Fushman, D. and Cowburn, D. (2001) In *Methods in Enzymology*, Vol. 339, James, T., Schmitz, U. and Doetsch, V. (Eds.), Academic Press, pp. 109–126.

Fushman, D. and Cowburn, D. (2002) In *Protein NMR for the Millenium (Biological Magnetic Resonance Vol 20)*, Krishna, N.R. and Berliner, L. (Eds.), Kluwer, pp. 53–78.

Fushman, D., Ohlenschlager, O. and Rüterjans, H. (1994) *J. Biomol. Struct. Dyn.*, **11**, 1377–1402.

Fushman, D., Tjandra, N. and Cowburn, D. (1998) *J. Am. Chem. Soc.*, **120**, 10947–10952.

Fushman, D., Tjandra, N. and Cowburn, D. (1999) *J. Am. Chem. Soc.*, **121**, 8577–8582.

Hall, J.B. and Fushman, D. (2003) *J. Biomol. NMR*, **27**, 261–275.

Hall, J.B. and Fushman, D. (2006) *J. Am. Chem. Soc.*, **128**, 7855–7870.

Korzhnev, D.M., Billeter, M., Arseniev, A.S. and Orekhov, V.Y. (2001) *Prog. NMR Spect.*, **38**, 197–266.

Kover, K.E. and Batta, G. (2001) *J. Magn. Reson.*, **150**, 137–146.

Kroenke, C.D., Rance, M. and Palmer, A.G.I. (1999) *J. Am. Chem. Soc.*, **121**, 10119–10125.

Kurita, J., Shimahara, H., Utsunomiya-Tate, N. and Tate, S. (2003) *J. Magn. Reson.*, **163**, 163–173.

Lipari, G. and Szabo, A. (1982) *J. Am. Chem. Soc.*, **104**, 4546–4559.

Loth, K., Pelupessy, P. and Bodenhausen, G. (2005) *J. Am. Chem. Soc.*, **127**, 6062–6068.

Oh, B.H., Westler, W.M., Darba, P. and Markley, J.L. (1988) *Science*, **240**, 908–911.

Palmer, A.G. III, Grey, M.J. and Wang, C. (2005) *Methods Enzymol.*, **394**, 430–465.

Pfeiffer, S., Fushman, D. and Cowburn, D. (2001) *J. Am. Chem. Soc.*, **123**, 3021–3036.

Vogeli, B., Kovacs, H. and Pervushin, K. (2004) *J. Am. Chem. Soc.*, **126**, 2414–2420.

Walker, O., Varadan, R. and Fushman, D. (2004) *J. Magn. Reson.*, **168**, 336–345.

Wylie, B.J., Franks, W.T. and Rienstra, C.M. (2006) *J. Phys. Chem. B Condens. Matter Mater. Surf. Interfaces Biophys.*, **110**, 10926–10936.

Xu, J., Millet, O., Kay, L.E. and Skrynnikov, N.R. (2005) *J. Am. Chem. Soc.*, **127**, 3220–3229.

Yip, G.N. and Zuiderweg, E.R. (2004) *J. Magn. Reson.*, **171**, 25–36.